

# Adducts of Tellurium Tetrachloride with Allyl Alcohol and Allyl Acetate: 1,2- vs 1,3-Addition and Structure and Dynamics of Te···O Interactions in Different Phases

Holger Fleischer,<sup>\*,†</sup> Bernd Mathiasch,<sup>†</sup> and Dieter Schollmeyer<sup>‡</sup>

*Institut für Anorganische Chemie und Analytische Chemie and Institut für Organische Chemie, Universität Mainz, Duesbergweg, D-55099 Mainz, Germany*

Received May 18, 2001

The compounds  $\text{Cl}_3\text{Te}[\text{CH}_2\text{CH}(\text{Cl})\text{CH}_2\text{O}(\text{H})\cdots]\cdot\text{Cl}_2\text{Te}[-\text{CH}_2\text{CH}(\text{Cl})\text{CH}_2\text{O}-]$  (**1**) and  $\text{Cl}_3\text{Te}[\text{CH}_2\text{CH}(\text{CH}_2\text{Cl})\text{OC}(\text{CH}_3)=\text{O}\cdots]$  (**2**) were prepared by the reaction of  $\text{TeCl}_4$  with allyl alcohol and allyl acetate, respectively. Their molecular and crystal structures were investigated by single-crystal X-ray analysis,  $^1\text{H}-^1\text{H}$ -NOESY experiments, IR spectroscopy, and ab initio geometry optimization. **1** is a composite compound, whose subunits  $\text{Cl}_2\text{Te}[-\text{CH}_2\text{CH}(\text{Cl})\text{CH}_2\text{O}-]$  (**1A**) and  $\text{Cl}_3\text{Te}[\text{CH}_2\text{CH}(\text{Cl})\text{CH}_2\text{O}(\text{H})\cdots]$  (**1B**) are linked in the solid state via  $\text{Te}\cdots\text{Cl}-\text{Te}$  and  $\text{O}\cdots\text{H}-\text{O}$  bridges. Both Te atoms are involved in similar five-membered rings, having a covalent  $\text{Te}-\text{O}$  bond in one case (**1A**) and a dative  $\text{Te}\cdots\text{O}$  bond in the other (**1B**). In the solid state, both Te atoms are pentacoordinate with pseudo-octahedral configurations. Formation of **2** is accompanied by a 3,2-migration of the acetate group, leading to a 1,3-addition of  $\text{TeCl}_4$  to allyl acetate and a six-membered ring via an intramolecular dative  $\text{Te}\cdots\text{O}$  interaction. In the solid state, single molecules of **2** are linked by weak  $\text{CH}_2\text{Cl}\cdots\text{Te}$  contacts, the Te atom being hexacoordinate with a distorted-octahedral configuration. Since reaction of **1** with acetyl chloride also gives **2**, the 1,3-addition product of  $\text{TeCl}_4$  with allyl acetate must be thermodynamically more stable than the corresponding 1,2-addition product, a conclusion that is supported by ab initio calculations. Ab initio calculations (MP2/LANL2DZP) for  $\text{Cl}_3\text{Te}[\text{CH}_2\text{CH}(\text{Cl})\text{CH}_2\text{O}(\text{H})\cdots]$  (**1B**) and **2** revealed strong  $n(\text{O})-\sigma^*(\text{Te}-\text{Cl})$  and Coulombic interactions for the  $\text{Te}\cdots\text{O}$  bonds, which are significantly longer in the isolated molecules than in the solid state. Multinuclear NMR spectroscopy and  $^1\text{H}-^1\text{H}$ -NOESY experiments show the cyclic structures to exist in solution as well, with little changes in their geometry compared to the solid state.

## Introduction

Electrophilic addition of  $\text{TeCl}_4$  to olefines is a well-studied reaction.<sup>1–8</sup> In contrast to  $\text{SeCl}_4$ ,  $\text{TeCl}_4$  usually reacts with only 1 equiv of an olefin, with regioselectivity according to Markovnikov and anti stereochemistry for the addition in most cases.<sup>9,10</sup> The molecular structures of some of these compounds have been reported.<sup>10</sup>

However, with some allylic systems different products and regioselectivities were observed.  $\text{TeCl}_4$  adds in an anti-Markovnikov fashion to both C=C bonds of  $\text{Y}(\text{CH}_2\text{-CH}=\text{CH}_2)_2$  (Y = O, S, NH, NMe), forming six-membered heterocyclic compounds with two chloromethylene groups at the 2- and 6-positions.<sup>11,12</sup> Reaction of diallylamides with  $\text{TeCl}_4$  afforded zwitterionic oxazolines,<sup>5</sup> while a rearrangement with a 3→2-shift of the acetyl group was postulated for the reactions of  $\text{TeCl}_4$  with allyl esters.<sup>6</sup> In contrast to the addition reaction, little is known about the molecular structure of the products and the coordination of tellurium in the adducts of  $\text{TeCl}_4$  with allylic systems, containing a donor atom in a  $\beta$ -position to the C=C double bond.<sup>5,8</sup> We report here the synthesis of the  $\text{TeCl}_4$  allyl alcohol adduct and investigations of its molecular structure and that of the  $\text{TeCl}_4$  allyl acetate adduct in the solid state and in solution by experimental methods, as well as structural and thermochemical studies for the isolated molecules by ab initio quantum chemical methods.

\* To whom correspondence should be addressed. E-mail: fleische@mail.uni-mainz.de. Fax: (+49) 6131 39 23351.

<sup>†</sup> Institut für Anorganische Chemie und Analytische Chemie.

<sup>‡</sup> Institut für Organische Chemie.

(1) de Moura Campos, M.; Petraghani, N. *Tetrahedron* **1962**, *18*, 521–526, 527–530.

(2) Halcon Research and Development Corp., New York, US Patent No. 4,271,090, 1979.

(3) Bergman, J.; Engman, L. *J. Am. Chem. Soc.* **1981**, *103*, 2715–2718.

(4) Bergman, J.; Engman, L. *J. Am. Chem. Soc.* **1981**, *103*, 5196–5200.

(5) Bergman, J.; Sidén, J.; Maartman-Moe, K. *Tetrahedron* **1984**, *40*, 1607–1610.

(6) Engman, L. *J. Am. Chem. Soc.* **1984**, *106*, 3977–3984.

(7) Engman, L. *Organometallics* **1989**, *8*, 1997–2000.

(8) Sundberg, M. R.; Laitalainen, T.; Bergman, J.; Uggla, R.; Matikaine, J.; Kaltia, S. *Inorg. Chem.* **1998**, *37*, 2786–2791.

(9) Albeck, M.; Tamari, T. *J. Organomet. Chem.* **1982**, *238*, 357–362.

(10)  $\text{TeCl}_4$  was reported to react with 2 equiv of ethene, propene, and butadiene: Arpe, H. J.; Kuckertz, H. *Angew. Chem.* **1971**, *83*, 81; *Angew. Chem., Int. Ed. Engl.* **1971**, *10*, 73.

(11) Migalina, Yu. V.; Staninets, V. I.; Lendel, V. G.; Balog, I. M.; Palyulin, V. A.; Koz'min, A. S.; Zefirov, N. S. *Khim. Get. Soedin.* **1977**, 58–62.

(12) Migalina, Yu. V.; Balog, I. M.; Lendel, V. G.; Koz'min, A. S.; Zefirov, N. S. *Khim. Get. Soedin.* **1978**, 1212–1214.

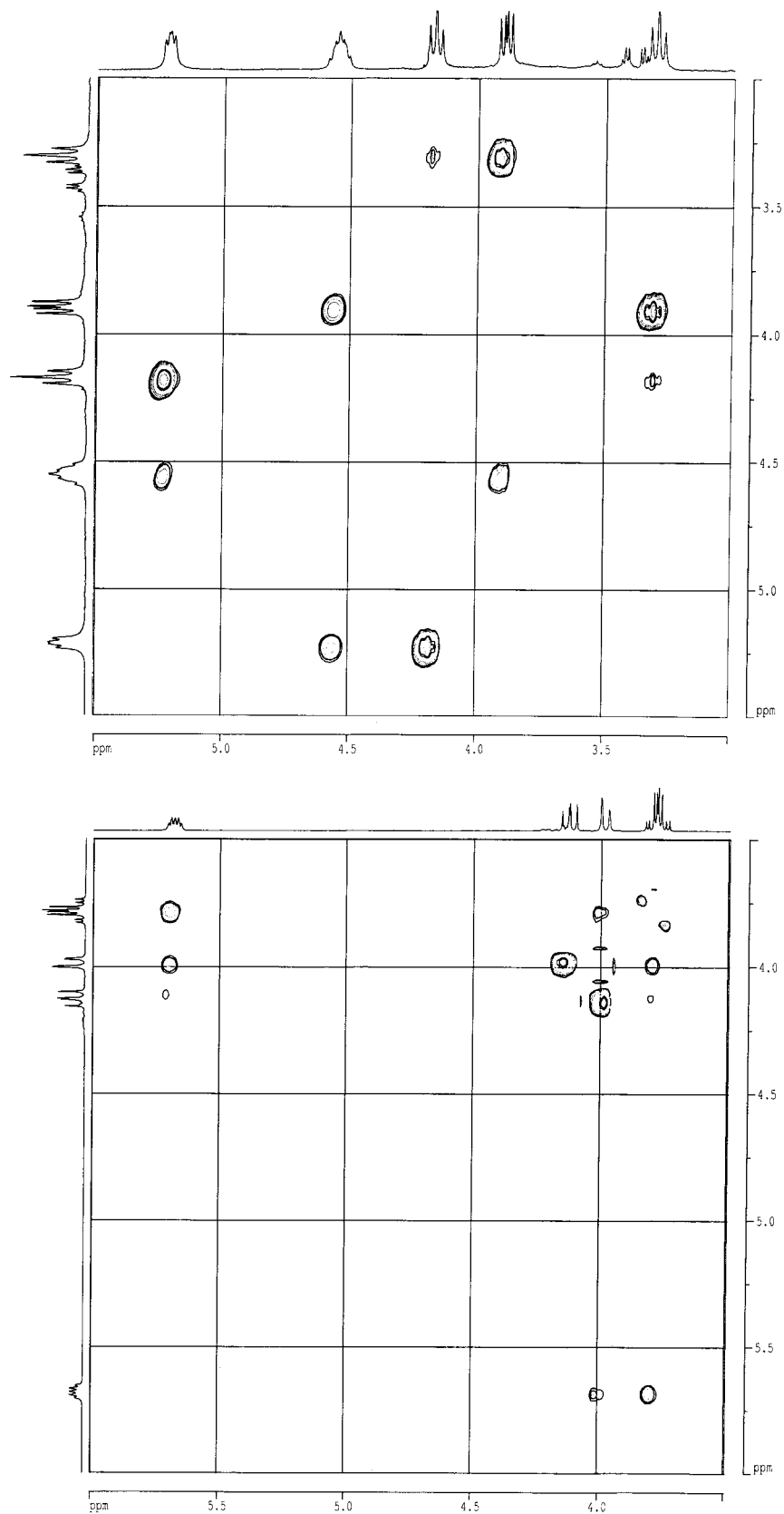


**Figure 1.**  $^1\text{H}$ - $^1\text{H}$ -NOESY spectrum of (a, top) **1** and (b, bottom) **2**.

### Results and Discussion

**Synthesis and Spectroscopy.** Two equivalents of allyl alcohol was added to  $\text{TeCl}_4$ , but it reacted only with 1 equiv to yield  $\text{Cl}_3\text{Te}[\text{CH}_2\text{CH}(\text{Cl})\text{CH}_2\text{O}(\text{H})\cdots]\cdot\text{Cl}_2$ -

$\text{Te}[-\text{CH}_2\text{CHClCH}_2\text{O}-]$  (**1**), according to eq 1.<sup>13</sup>



**1** represents a composite product that is formed by

**Table 1. Relative NOE Buildup Rates and H...H Distances (in Å) from  $^1\text{H}$ - $^1\text{H}$ -NOESY Experiments and from MP2/LANL2DZP Geometry Optimizations.<sup>a</sup> (a) for **1**, **1A** and **1B** (b) for **2****

(a) Compounds <b>1</b> , <b>1A</b> , and <b>1B</b>				
	rel NOE buildup rate	NOE dist for <b>1</b> <sup>b</sup>	ab initio <b>1A</b>	ab initio <b>1B</b>
H <sup>A</sup> ...H <sup>B</sup>	0.952	1.819	1.809	1.819
H <sup>X</sup> ...H <sup>Y</sup>	1.000	1.804	1.805	1.803
H <sup>B</sup> ...H <sup>M</sup>	0.259	2.260	2.441	2.400
H <sup>M</sup> ...H <sup>Y</sup>	0.191	2.377	2.482	2.447
H <sup>A</sup> ...H <sup>X</sup>	0.063	2.860	2.635	2.813

(b) Compound <b>2</b>			
	rel NOE buildup rate	NOE dist for <b>2</b> <sup>b</sup>	ab initio
H <sup>A</sup> ...H <sup>B</sup>	1.000	1.809	1.809
H <sup>A</sup> ...H <sup>X</sup>	0.043	3.054	3.088
H <sup>B</sup> ...H <sup>X</sup>	0.149	2.489	2.554

<sup>a</sup> Numbering scheme according to Chart 1. <sup>b</sup> NOE distances all refer to H<sup>A</sup>...H<sup>B</sup>, which is independent of C-C torsions. It was set equal to the MP2/LANL2DZP optimized distances in **1B** and **2**, respectively.

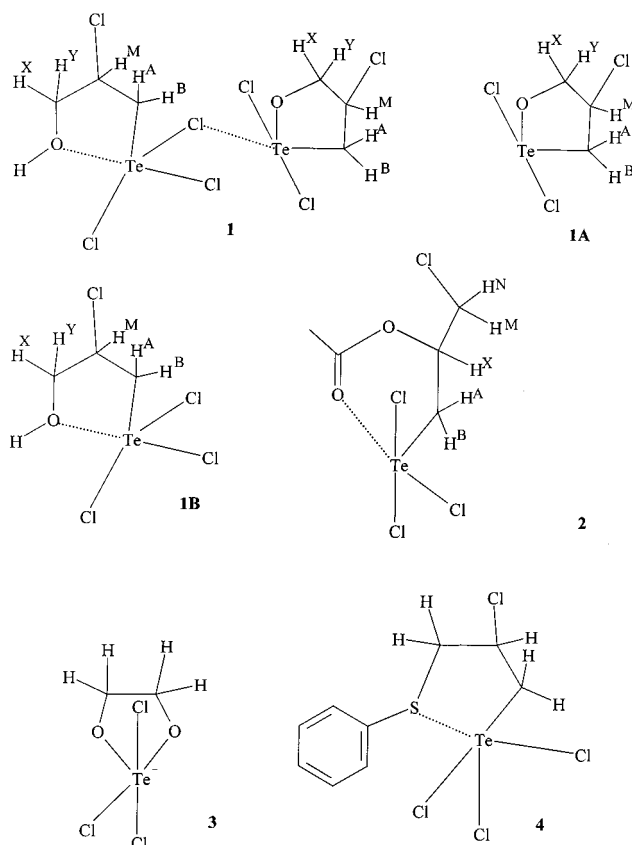
the subunits Cl<sub>2</sub>Te[−CH<sub>2</sub>CH(Cl)CH<sub>2</sub>O−] (**1A**) and Cl<sub>3</sub>Te[CH<sub>2</sub>CH(Cl)CH<sub>2</sub>O(H)⋯] (**1B**). An asymmetric C atom is generated in the course of the addition of TeCl<sub>4</sub> to allyl alcohol, and due to the absence of chiral discrimination, a racemic mixture of **1** is formed. Since both **1A** and **1B** contain an asymmetric C atom, formation of *RR/SS* and *RS/SR* diastereomers of **1** is possible (see Crystal and Molecular Structures). **1** is only slightly soluble in nonpolar solvents but dissolves fairly well in DMSO, a fact attributed to the strong intermolecular forces in the solid state.

The  $^1\text{H}$  NMR spectrum of **1** in DMSO-*d*<sub>6</sub> exhibits six different signals: a broad singlet due to the −OH group, a multiplet representing the proton in −CHCl−, two doublets of doublets and two triplets for the −OCH<sub>2</sub>− and −TeCH<sub>2</sub>− groups. A  $^1\text{H}$ - $^1\text{H}$ -COSY experiment reveals the triplets to be superpositions of doublets of doublets, due to nearly equal values of  $^2J(\text{H},\text{H})$  and  $^3J(\text{H},\text{H})$ . As  $^3J(\text{H},\text{H})$  couplings depend on the dihedral angle of the HCCH unit,<sup>14</sup> we assigned the large couplings to H atoms in an anti conformation and the small couplings to H atoms in a gauche conformation. This was confirmed by a  $^1\text{H}$ - $^1\text{H}$ -NOESY spectrum, from which averaged H...H distances could be obtained (see Figure 1a and Table 1a). Apart from the signal of the −OH group, the spectrum represents the ABMX<sub>2</sub>-type spin system of a −CH<sub>2</sub>CH(Cl)CH<sub>2</sub>O− moiety (see Chart 1). As two different kinds of −CH<sub>2</sub>CH(Cl)CH<sub>2</sub>O− moieties—one in **1A** and one in **1B**—are present, a rapid interconversion of the two must take place in order to lead to an averaged set of signals. This view is supported by the  $^{125}\text{Te}$  NMR spectrum of **1**. Two different signals are expected, but at 25 °C none was observed, presumably due to extreme broadening by chemical exchange. At 70 °C, a very broad signal appeared at 1416 ppm. These results suggest that **1** dissociates into **1A** and **1B**

(13) Under the same conditions, TeCl<sub>4</sub> did not add to allyl bromide, but an exchange of Cl and Br atoms occurred. When a 1:1 mixture of ClTe(O<sup>i</sup>Pr)<sub>3</sub> and allyl alcohol were refluxed in benzene and the volatile products distilled off, no addition to the C=C bond occurred, but one O<sup>i</sup>Pr ligand was exchanged for a OCH<sub>2</sub>CH=CH<sub>2</sub> ligand. Allyl bromide is thus less reactive than allyl alcohol, and ClTe(O<sup>i</sup>Pr)<sub>3</sub> is a weaker electrophile than TeCl<sub>4</sub>.

(14) Karplus, M. *J. Am. Chem. Soc.* **1963**, *85*, 2870–2871.

**Chart 1. Structural Formulas of Compounds Discussed in the Present Work**



on dissolution in DMSO, and the two different molecules are converted into each other by H<sup>+</sup> and Cl<sup>−</sup> transfer. Since the signals of the ABMX<sub>2</sub>-type spin system are well resolved, the −CH<sub>2</sub>CH(Cl)CH<sub>2</sub>O fragment cannot be much affected by this chemical exchange and the relatively rigid ring structures of **1** are kept intact.

Cl<sub>3</sub>Te[CH<sub>2</sub>CH(CH<sub>2</sub>Cl)OC(CH<sub>3</sub>)=O⋯] (**2**) was prepared according to the method of Engman.<sup>6</sup> Again an asymmetric C atom is generated in the course of the reaction and a racemic mixture of **2** was obtained. In contrast to **1**, **2** dissolves well in chloroform. A detailed discussion of the  $^1\text{H}$  NMR spectrum of **2** was already given by Engman. The signals of H<sup>M</sup> and H<sup>N</sup> (see Chart 1), which are merged at room temperature (multiplet, 3.82–3.73 ppm), resolved at −40 °C into two doublets of doublets (dd), due to  $^2J(\text{H}^{\text{M}},\text{H}^{\text{N}})$ ,  $^3J(\text{H}^{\text{M}},\text{H}^{\text{X}})$ , and  $^3J(\text{H}^{\text{N}},\text{H}^{\text{X}})$  coupling, respectively. The resolution of the signals is explained by “freezing” of the rotation of the −CH<sub>2</sub>Cl group at lower temperatures. The doublet of doublets at higher field exhibits the larger  $^3J(\text{H},\text{H})$  coupling to H<sup>X</sup> and is subsequently assigned to H<sup>N</sup>, as the torsional angle  $\tau(\text{H}^{\text{N}}\text{CCH}^{\text{X}})$  is close to an anti conformation (see Chart 1). Assignment of the  $^{13}\text{C}$  NMR signals was accomplished by a DEPT experiment.

Between +20 and −40 °C, the  $^{125}\text{Te}$  NMR signal does not depend on the temperature. A constant environment of the pentacoordinate Te atom in **2** over that temperature range and, hence, a strong Te⋯O interaction is inferred from this result. This is in accordance with the well-resolved multiplets of H<sup>A</sup>, H<sup>B</sup>, and H<sup>X</sup> in the  $^1\text{H}$  NMR spectrum, implying rather constant dihedral angles H<sup>A</sup>CCH<sup>X</sup> and H<sup>B</sup>CCH<sup>X</sup> and, hence, excluding a

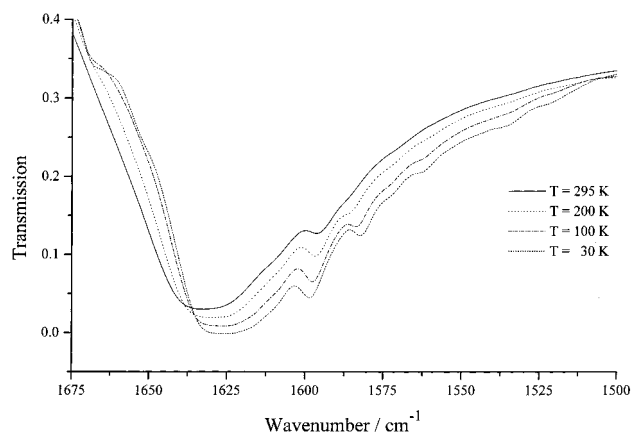


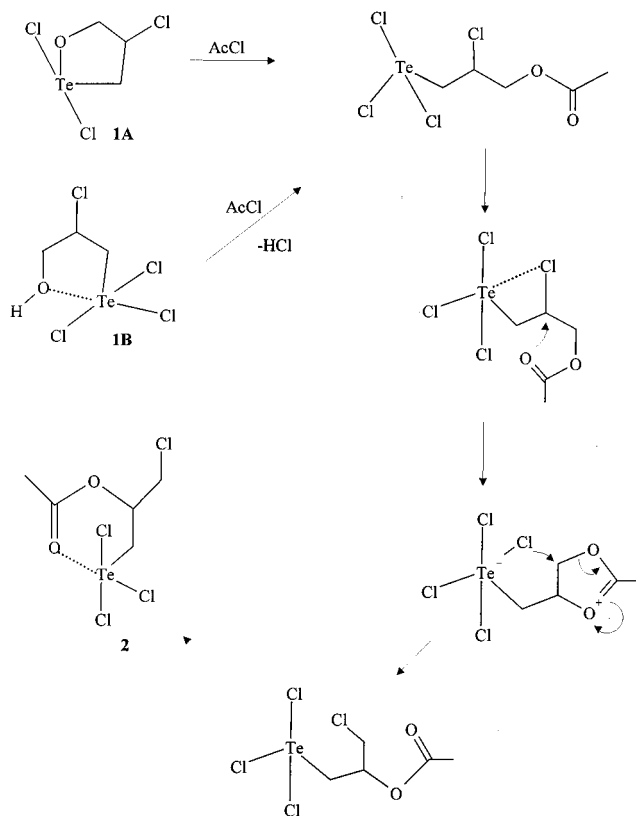
**Figure 2.**  $\nu(\text{C}=\text{O})$  bands from the VT IR spectra of **2**.

cleavage of the  $\text{Te}\cdots\text{O}$  bond and a breakdown of the ring structure of **2**.

In comparison to allyl acetate, the frequency of the carbonylic stretching vibration,  $\nu(\text{C}=\text{O})$ , in **2** is shifted to lower wavenumbers by  $115\text{ cm}^{-1}$ , a fact attributed to a weakening of the  $\text{C}=\text{O}$  bond by the intramolecular  $\text{Te}\cdots\text{O}$  interaction.<sup>6</sup> The model of the anharmonic, diatomic oscillator predicts its IR band to exhibit a negative temperature gradient, i.e. a shift to lower wavenumbers with increasing temperature, due to increasing population of vibrational states with  $\nu > 0$ , and the bond between the two atoms becomes weaker. It is thus interesting that  $\nu(\text{C}=\text{O})$ , in the range between 30 and 300 K, exhibits a distinctly positive temperature gradient (see Figure 2). This is explained by its coupling to the  $\text{Te}\cdots\text{O}$  oscillation. The  $\text{Te}\cdots\text{O}$  bond becomes stronger at lower temperature at the cost of the  $\text{C}=\text{O}$  bond, and this overcompensates the strengthening of the latter.

Engman reported that the product from the reaction of  $\text{TeCl}_4$  with allyl alcohol, which was not identified as **1**, can be converted into compound **2** if it is treated with acetyl chloride.<sup>6</sup> If **1** can be converted into **2** by this procedure, a 2,3-migration of the acetyl group must occur and it would be very likely that **1** is identical with Engman's product. When acetyl chloride was added to a suspension of **1** and  $\text{CHCl}_3$ , the solid immediately dissolved. A  $^1\text{H}$  NMR spectrum taken after 3 h of refluxing shows the formation of **2** among several other products. When the mixture was refluxed for another 6 h, the amount of **2** increased and those of the other products decreased. Hence, the  $\text{Te}-\text{O}$  bonds in **1** are cleaved by acetyl chloride, as would be expected from the reaction of tellurium(IV) alkoxides with acetyl chloride,<sup>15</sup> and subsequently a 3,2-shift of the acetyl group occurs, but the overall reaction is slower than formation of **2** from  $\text{TeCl}_4$  and allyl acetate. A reasonable mechanism is depicted in Scheme 1. Different from the reaction of  $\text{TeCl}_4$  with allyl acetate (see Figure 2 in ref 6), the 3,2-shift of the acetyl group in the reaction of **1** with acetyl chloride does not proceed via a cationic intermediate but requires an  $\text{S}_{\text{N}}2$ -type mechanism. The heterolytic cleavage of the  $\text{C}-\text{Cl}$  bond might be supported by the  $\text{Te}$  atom in a  $\beta$ -position, to which the  $\text{Cl}^-$  ion can coordinate. Hence, the mobility of the acetyl group allows the conversion of the 1,2-adduct into the

### Scheme 1. Proposed Mechanism for the Formation of **2** from **1**



thermodynamically more stable 1,3-adduct of  $\text{TeCl}_4$  with allyl acetate. Results from ab initio calculations comparing the relative thermodynamic stabilities of the 1,2- and 1,3-adducts are given further down.

**Crystal and Molecular Structures.** The molecular structures of **1** and **2** in the solid state are given in Figures 3 and 4, respectively. Selected structural parameters of **1**, **1A**, **1B**, and **2** are given in Tables 2 and 3.

The XRD structures reveal different paths for the reactions of  $\text{TeCl}_4$  with allyl alcohol and allyl acetate as well as different modes of intramolecular  $\text{Te}\cdots\text{O}$  coordination in **1** and **2**. In the solid-state structure of **1**, units of **1A** and **1B**—the former being an  $\text{HCl}$ -elimination product of the latter—interact with each other via alternating  $\text{Te}-\text{Cl}\cdots\text{Te}$  and  $\text{O}-\text{H}\cdots\text{O}$  bridges. C31 exhibits 75% *S* and 25% *R* configuration, while C32 is 70% *R* and 30% *S* configured, and vice versa for the second molecule of **1** in the unit cell. **2** forms chains via  $\text{C}-\text{Cl}\cdots\text{Te}$  contacts between molecules with alternating *R*- and *S*-configured C2 atoms.

**1A** and **1B** allow for an interesting comparison between the two five-membered rings, differing only in the nature of the  $\text{Te}-\text{O}$  bonds: i.e., covalent in **1A** and dative in **1B**.<sup>16</sup> As would be expected, the dative  $\text{Te11}\cdots\text{O11}$  bond is much longer and hence weaker than the covalent  $\text{Te12}-\text{O12}$  bond, in the solid state as well as in the ab initio optimized molecular structures. In

(16) "Covalent" and "dative" bonds are distinguished according to Haaland (Haaland, A. *Angew. Chem.* **1989**, *101*, 1017–1032; *Angew. Chem., Int. Ed. Engl.* **1989**, *28*, 992–1007); i.e., bonds are classified as "covalent" or "dative", if least-energy cleavage is homolytic or heterolytic, respectively. According to this criterion,  $\text{Te12}-\text{O12}$  is covalent and  $\text{Te11}\cdots\text{O11}$  is dative, independent of their actual length.

(15) Fleischer, H.; Schollmeyer, D. *Inorg. Chem.* **2001**, *40*, 324–328.



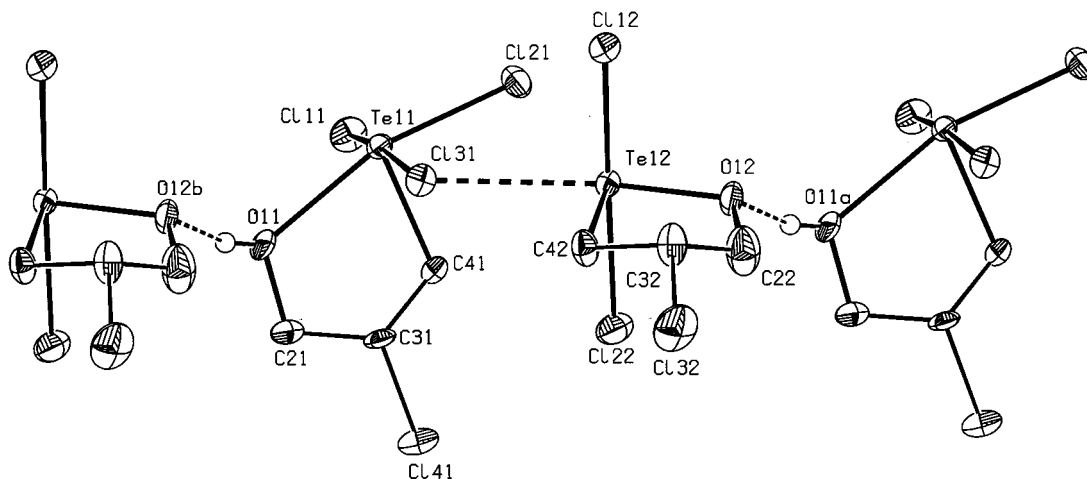


**Figure 3.** Molecular structure of **1** in the solid state. Hydrogen atoms bound to carbon atoms are omitted for clarity. Displacement ellipsoids are at the 50% probability level.

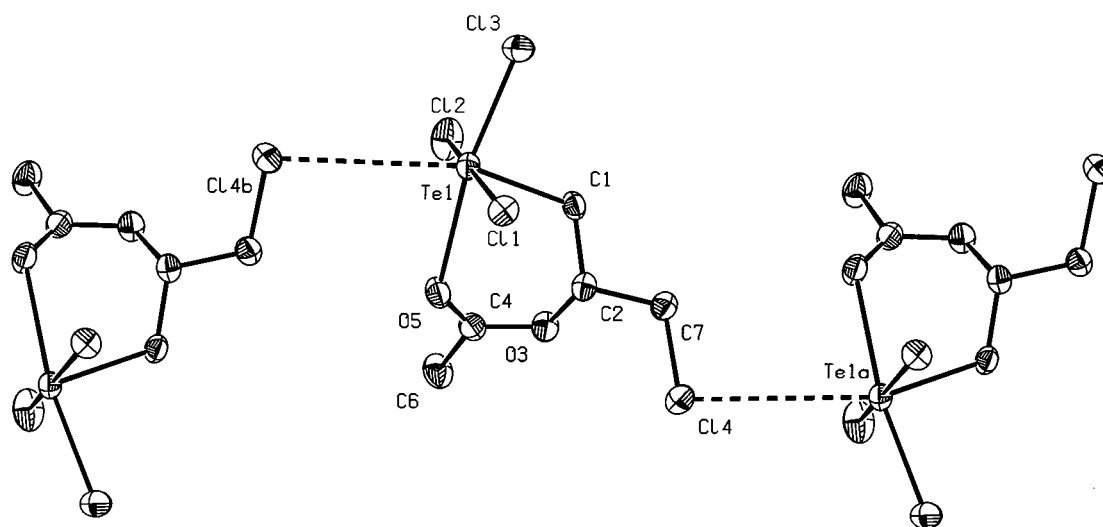


**Figure 4.** Molecular structure of **2** in the solid state. Hydrogen atoms are omitted for clarity. Displacement ellipsoids are at the 50% probability level.

accordance with ring strains, the angle O12–Te12–C42 is 10° wider than O11··Te11–C41. No other corresponding parameters in the two rings show such differences. Te11··O11 is shorter and hence stronger in the solid state than in the isolated molecule, a well-known feature of dative bonds.<sup>17,18</sup> In contrast, Te12–O12 is longer in the solid-state structure of **1** than in the isolated **1A**, a fact attributed to the Te12··Cl31 interaction opposite to Te12–O12 and the O12··H hydrogen bond, both of which are present in **1** but not in **1A**, and both weaken Te12–O12.

The strength of the Te11–Cl31··Te12 bridge can be judged by the symmetry parameter  $s = [d(\text{Te}\cdots\text{Cl}) - d(\text{Te}-\text{Cl})]/[d(\text{Te}\cdots\text{Cl}) + d(\text{Te}-\text{Cl})]$ .<sup>15,19</sup> The smaller the value of  $s$ , the more symmetric and—having a comparable sum of distances,  $d(\text{Te}\cdots\text{Cl}) + d(\text{Te}-\text{Cl})$ —the stronger the bridge. **1** ( $s = 0.035$ ) is an intermediate case between rather weak bridges, as for example in phenoxatellurin 10,10-dichloride ( $s = 0.136$ – $0.167$ ),<sup>20</sup> and

symmetric bridges, as in the TeCl<sub>4</sub>–ethene adduct (2-chloroethyl)trichlorotellurane ( $s = 0$ ).<sup>21</sup>

As a consequence of the Te12··Cl31 contact, Te11–Cl31 is longer, and due to a reduced trans effect, Te11–Cl11 is shorter in **1** than in **1B**. The ab initio optimized geometries clearly reveal that the mutual trans effects of Te11–Cl11 and Te11–Cl31 in **1B** and Te12–Cl12 and Te12–Cl22 in **1A** are stronger than the trans effect of Te11··O11 on Te11–Cl21. Te11–C41 and Te12–C42 are trans to the lone pair and of similar lengths in **1**, **1A**, and **1B**. The configurations of Te11 and Te12 in **1** are in accordance with Alcock's rules for secondary bonding<sup>22</sup> and are best described as distorted  $\psi$ -octahedral, with the lone pair occupying the sixth position. In accordance with the VSEPR principle, distortion of the bonds is away from the lone pair (see Table 2 for the respective bond angles).

For the interconversion of **1A** and **1B**, a transfer of Cl31 from Te11 to Te12 and a proton transfer from O11 to O12 are necessary, accompanied by a configurational

(17) Leopold, K. R.; Canagaratna, M.; Phillips, J. A. *Acc. Chem. Res.* **1997**, *30*, 57–64.

(18) Hensen, K.; Stumpf, T.; Bolte, M.; Näther, C.; Fleischer, H. *J. Am. Chem. Soc.* **1998**, *120*, 10402–10408.

(19) Landrum, G. A.; Hoffmann, R. *Angew. Chem.* **1998**, *110*, 1889–1892; *Angew. Chem., Int. Ed.* **1998**, *37*, 1887–1890.

(20) Korp, J. D.; Bernal, I.; Turley, J. C.; Martin, G. E. *Inorg. Chem.* **1980**, *19*, 2556–2560.

(21) Kobelt, D.; Paulus, E. F. *Angew. Chem.* **1971**, *83*, 81–82; *Angew. Chem., Int. Ed. Engl.* **1971**, *10*, 73–74.

(22) Alcock, N. W. *Adv. Inorg. Radiochem.* **1972**, *15*, 1–58.

**Table 2. Selected Structural Parameters (Atomic Distances in Å, Angles in deg) from MP2/LANL2DZP Optimized Geometries of Cl<sub>2</sub>Te(-CH<sub>2</sub>CH<sub>2</sub>CH<sub>2</sub>O-) (1A) and Cl<sub>3</sub>Te(-CH<sub>2</sub>CH<sub>2</sub>CH<sub>2</sub>O(H)...) (1B) and XRD Geometry of 1<sup>a</sup>**

	<b>1</b>	<b>1A</b>	<b>1B</b>
Te12-Cl12	2.495(2)	2.495	
Te12-Cl22	2.514(2)	2.460	
Te12-O12	1.980(4)	1.944	
Te12-C42	2.121(6)	2.133	
Te12...Cl31	2.918(2)		
O12-C22	1.426(7)	1.451	
C22-C32	1.488(11)	1.533	
C32-C42	1.544(10)	1.539	
Cl12-Te12-Cl22	173.6(1)	172.2	
C42-Te12-Cl12	86.7(2)	86.1	
C42-Te12-Cl22	87.3(2)	87.2	
C42-Te12-O12	84.4(2)	87.1	
C42-Te12...Cl31	84.1(2)		
Cl31...Te12-O12	168.5(2)		
Te12-O12-C22	112.6(4)	110.3	
O12-C22-C32	113.3(6)	107.9	
C22-C32-C42	109.6(7)	109.6	
C32-C42-Te12	105.0(5)	101.7	
Te11-Cl11	2.378(2)		2.465
Te11-Cl21	2.361(2)		2.350
Te11-Cl31	2.720(2)		2.500
Te11...O11	2.386(4)		2.545
Te11-C41	2.141(5)		2.136
O11-C21	1.433(7)		1.453
C21-C31A	1.474(11)		1.524
C31A-C41	1.492(10)		1.524
Cl11-Te11-Cl31	173.0(1)		168.5
Cl21-Te11...O11	165.1(1)		163.6
C41-Te11-Cl11	89.5(2)		84.6
C41-Te11-Cl21	90.7(2)		90.9
C41-Te11-Cl31	83.6(2)		86.5
C41-Te11...O11	74.4(2)		74.8
Te11...O11-C21	113.6(3)		197.1
O11-C21-C31A	107.3(6)		104.6
C21-C31A-C41	114.9(7)		112.0
C31A-C41-Te11	111.1(4)		110.9
Te11-Cl31...Te12	107.3(1)		

<sup>a</sup> The numbering scheme of the atoms is according to that in Figure 3. MP2/LANL2DZP atomic distances refer to an *r<sub>e</sub>* structure.

rearrangement of Te11: i.e., Cl21 moving to the former position of Cl31. Since configurationally unrestrained tellurium(IV) exhibits rather small energy barriers for intramolecular rearrangements,<sup>23</sup> the steps just outlined would give a reasonable mechanism for the observed quick interconversion of **1A** and **1B** in solution.

Apart from Cl4, **1B** is isoelectronic with trichloro-(ethane-1,2-diolato-*O,O'*)tellurate(IV) (**3**), the anionic part of the immunomodulating compound AS-101 (see Chart 1).<sup>24</sup> The lengths of the two Te-O bonds in AS-101, 1.964 and 1.939 Å, are within the range of Te-O single bonds and thus are significantly shorter than Te11...O11 in **1**. As a consequence, the Te-Cl bond trans to the Te-O bond is much longer in AS-101 (2.711 Å) than in **1**.

The geometry of the coordination polyhedron around Te11 is similar to that of the Te atom in compound **4** (see Chart 1), as can be seen from the Te-Cl (2.382(2), 2.486(2), and 2.497(2) Å) and the Te-C (2.131(7) Å) distances and the Cl-Te-Cl (92.6(1), 90.6(1), and 166.7-(1)°) and S...Te-C (77.9(2)°) angles of the latter.<sup>8</sup>

Most bond lengths and angles of **2** in the solid state are well-reproduced by the MP2/LANL2DZP optimized geometry, which shows that intermolecular forces do not lead to significant distortion of the molecular structure. The C-C and C-O bonds are slightly longer in the

**Table 3. Selected Structural Parameters (Atomic Distances in Å, Angles in deg) from Single-Crystal XRD and ab Initio MP2/LANL2DZP Geometry Optimizations of 2<sup>a</sup>**

	XRD	ab initio
Te1-Cl1	2.498(1)	2.469
Te1-Cl2	2.497(1)	2.492
Te1-Cl3	2.354(1)	2.353
Te1...Cl4	3.731(1)	
Te1...O5	2.441(2)	2.510
Te1-C1	2.136(3)	2.137
C1-C2	1.500(5)	1.523
C2-C7	1.503(4)	1.522
C4-C6	1.469(5)	1.496
C4-O3	1.332(4)	1.337
C4-O5	1.219(4)	1.243
C7-Cl4	1.790(3)	1.776
O5-C4-O3	122.8(3)	122.3
C6-C4-O5	124.0(3)	124.3
C6-C4-O3	113.2(3)	113.5
C4-O5...Te1	122.2(2)	116.0
C4-O3-C2	117.0(3)	115.6
Cl1-Te1-Cl2	170.0(1)	167.7
Cl1-Te1-Cl3	92.7(1)	93.4
Cl2-Te1-Cl3	92.1(1)	92.7
O5...Te1-Cl3	169.3(1)	169.6
C1-Te1-Cl1	84.2(1)	83.8
C1-Te1-Cl2	87.1(1)	85.6
C1-Te1-Cl3	89.8(1)	90.0
Te1...Cl4-C7	101.4(1)	
Te1...O5-C4-O3	45.0(4)	51.0
Cl4-C7-C2-C1	170.3(2)	176.2

<sup>a</sup> The numbering of the atoms is according to Figure 4. MP2/LANL2DZP atomic distances refer to an *r<sub>e</sub>* structure.

isolated molecule, but the most significant difference is the dative Te1...O5 bond, which, as in **1**, is longer in the isolated molecule than in the solid state. It is further noteworthy that the intermolecular Te...Cl contact is more than 0.8 Å longer in **2** than in **1** and, as a consequence, C7-Cl4, in contrast to Te11-Cl31, is hardly lengthened by such an interaction. The rather weak intermolecular interactions in **2** compared to those in **1** are seen to be responsible for its better solubility in chloroform. In the solid state, **2** exhibits a longer dative Te...O bond than **1**. Their similarity in the isolated molecules is accidental, as carbonylic and alcoholic O atoms are different in their electronic properties, as are ring strains in five- and six-membered rings. The intramolecular Te...O distances in **1** and **2** are short compared to other Te(IV) compounds with similar interactions (cf. ref 25).

**Ab Initio Thermochemistry and NBO Analysis.** HF/LANL2DZP//HF/LANL2DZP (MP2/LANL2DZP//MP2/LANL2DZP) thermochemical calculations reveal  $\Delta H^{298} = 48.4$  (51.9) kJ mol<sup>-1</sup> and  $\Delta G^{298} = 11.2$  (13.2) kJ mol<sup>-1</sup> for reaction 2; i.e., concerning the isolated molecules,



**1B** is stable with respect to dissociation into **1A** and HCl. **1A** can be regarded to act simultaneously as a Brønsted base and a Lewis acid toward HCl. In the solid state there are hydrogen and chlorine bridges linking adjacent molecules of **1A** and **1B** (see Figure 3). Accord-

(23) Denney, D. B.; Denney, D. Z.; Hammond, P. J.; Hsu, Y. F. *J. Am. Chem. Soc.* **1981**, *103*, 2340-2347.

(24) Sredni, B.; Caspi, R. R.; Klein, A.; Kalechman, Y.; Danzinger, Y.; Ben Ya'akov, M.; Tamari, T.; Shalit, F.; Albeck, M. *Nature* **1987**, *330*, 173-176.

(25) Abid, K. Y.; Al-Salim, H.; Greaves, W. R.; McWhinnie, W. R.; West, A. A.; Hamor, T. A. *J. Chem. Soc., Dalton Trans* **1989**, 1697-1703.

**Table 4.** MP2/LANL2DZP Natural Atomic Charges of Selected Atoms of **1A**, **1B**, **2**, and **4**

	<b>1A</b>	<b>1B</b>	<b>2</b>	<b>4<sup>a</sup></b>
Te	+1.98	+1.80	+1.84	+1.73
C <sub>Te</sub>	-0.73	-0.74	-0.77	-0.68
E <sub>Te</sub> <sup>b</sup>	-0.95	-0.87	-0.83	+0.30
Cl <sub>Te</sub> <sup>trans c</sup>		-0.43	-0.44	-0.46
Cl <sub>Te</sub> <sup>cis c,d</sup>	-0.60	-0.60	-0.59	-0.60

<sup>a</sup> Taken from ref 8. Charges were calculated at the MP2 level with a basis set similar to that used in the present work. <sup>b</sup> **1A**, **1B**, and **2**, E = O bound to Te; **4**, E = S. <sup>c</sup> Trans and cis refer to position relative to E in a  $\psi$ -octahedron at Te. <sup>d</sup> Average value.

ing to HF/LANL2DZP//HF/LANL2DZP thermochemical calculations, these bridges have similar strengths, the energies of dissociation being 30.0 kJ mol<sup>-1</sup> for **1B**-OH $\cdots$ **1A** and 31.4 kJ mol<sup>-1</sup> for **1B**-Cl $\cdots$ **1A**.<sup>26</sup> Hence, the energy gain by formation of these bridges between **1A** and **1B** just compensates the energy necessary for the formation of **1A** from **1B** and thus rationalizes experimental findings.

(MP2/LANL2DZP//MP2/LANL2DZP) thermochemical calculations show an exothermal conversion of the 1,2-adduct of TeCl<sub>4</sub> and allyl acetate into the corresponding 1,3-adduct, with  $\Delta H^\ddagger_{98} = -26.2$  kJ mol<sup>-1</sup>. Hence the 1,3-adduct is calculated to be thermodynamically more stable, in accordance with the fact that the 1,3- and not the 1,2-adduct is formed from **1** and acetyl chloride (vide infra). The calculated Te $\cdots$ O distance in the 1,2-adduct (2.666 Å) is significantly longer than the corresponding distances in **1B** and **2**.

According to second-order perturbation calculations in an NBO basis,<sup>27,28</sup> interaction energies between the lone pairs of the O atom and the  $\sigma^*$  orbital of the Te-Cl bond trans to Te $\cdots$ O are 96.1 and 108.2 kJ mol<sup>-1</sup> for **1B** and **2**, respectively, indicating strong Te $\cdots$ O bonds. The respective energy for the 1,2-adduct of TeCl<sub>4</sub> with allyl acetate is only 39.0 kJ mol<sup>-1</sup>, thus rationalizing the thermodynamic favor for the 1,3-addition product in terms of stronger intramolecular Te $\cdots$ O interactions.

The natural atomic charges of alike atoms agree quite well among the molecules depicted in Table 4, with two exceptions. The tetracoordinated Te atom in **1A** is distinctly more positively charged than the pentacoordinated Te atoms in the other compounds, and the O atom covalently bound to Te carries a higher negative charge than the O atoms with a dative Te $\cdots$ O bond. Especially small differences in the atomic charges occur between **1B** and **4**, a fact attributed to their similar molecular structures. Interestingly, the C<sub>Te</sub> atoms are more negatively charged than the Cl atoms, and the Cl atoms cis to the donor atom E carry a higher negative charge than those trans to it. The rather high positive natural charge of the Te atoms and the pronounced negative charge of the donor atoms E indicate distinct ionic contributions to the Te $\cdots$ E bonds, thus explaining their stabilization in the solid state.

### Conclusion

The adduct Cl<sub>3</sub>Te[CH<sub>2</sub>CH(Cl)CH<sub>2</sub>O(H) $\cdots$ ]·Cl<sub>2</sub>Te[-CH<sub>2</sub>CH(Cl)CH<sub>2</sub>O-] (**1**) is the main product of the reaction of TeCl<sub>4</sub> with allyl alcohol. The driving force for the elimination of HCl from Cl<sub>3</sub>Te[CH<sub>2</sub>CH(Cl)-

CH<sub>2</sub>O(H) $\cdots$ ] (**1A**), which gives Cl<sub>2</sub>Te[-CH<sub>2</sub>CH(Cl)-CH<sub>2</sub>O-] (**1B**), is the formation of strong O-H $\cdots$ O and Te-Cl $\cdots$ Te bridges in the solid state. The formation of **2**, from TeCl<sub>4</sub> and allyl acetate and from **1** and acetyl chloride, shows that a 3,2-shift of the acetyl group takes place and the 1,3-adduct is thermodynamically favored over the 1,2-adduct.

The dative Te $\cdots$ O bond is much more influenced by the molecular environment than the covalent Te-O bond. For **1** and for **2**, the Te $\cdots$ O bonds are significantly shorter in the solid state than in the ab initio optimized geometry of the isolated molecules, presumably due to stabilizing effects by a polar environment.

Apart from the differences in the Te $\cdots$ O bonds, the ring structures of **1** and also of **2** are similar in the solid state, in solution, and in the isolated molecule as calculated ab initio, showing the high strengths of the dative Te $\cdots$ O bonds which prevent cleavage of the rings. Especially the interconversion of the environments of the two Te atoms in **1** is achieved without ring opening. The <sup>125</sup>Te signal of **2** exhibits only a very small temperature gradient, which suggests a rather constant environment of the Te atom over a wide temperature range.

### Experimental Section

**General Methods.** TeCl<sub>4</sub> was handled under an inert gas atmosphere or under vacuum, using carefully dried glassware and solvents purified according to standard procedures. NMR: B<sub>1</sub>(<sup>1</sup>H) = 400.0 MHz, B<sub>1</sub>(<sup>13</sup>C) = 100.577 MHz, B<sub>1</sub>(<sup>125</sup>Te) = 126.387 MHz. Standards: TMS (<sup>1</sup>H, <sup>13</sup>C) and Te(CH<sub>3</sub>)<sub>2</sub> (<sup>125</sup>Te). IR: Mattson Galaxy 2030 FTIR, resolution 4 cm<sup>-1</sup> (room temperature), and Bruker IFS-66 v/s FT IR with Oxford Optistat continuous flow, resolution 2 cm<sup>-1</sup> (low temperature). Band assignment was supported by MP2/LANL2DZP calculated vibrational frequencies, which were scaled by a factor of 0.94.

Cl<sub>3</sub>Te[CH<sub>2</sub>CH(Cl)CH<sub>2</sub>O(H) $\cdots$ ]·Cl<sub>2</sub>Te[-CH<sub>2</sub>CH(Cl)-CH<sub>2</sub>O] (**1**). Allyl alcohol (1.37 g, 23.59 mmol) was slowly added to a stirred suspension of TeCl<sub>4</sub> (3.03 g, 11.25 mmol) in 15 mL of CCl<sub>4</sub>. TeCl<sub>4</sub> was initially dissolved, but after the reaction mixture was refluxed for 30 min, a yellow oil separated, from which a white, powdery solid was obtained at -20 °C. The solid was isolated and dried in vacuo.

Yield: 3.47 g, 94%. Mp: 147 °C dec. Anal. Calcd for C<sub>6</sub>H<sub>11</sub>-Cl<sub>7</sub>O<sub>2</sub>Te<sub>2</sub> (fw = 618.50): C, 11.65; H, 1.79. Found: C, 11.58; H, 2.08. <sup>1</sup>H NMR (DMSO-*d*<sub>6</sub>, 25 °C;  $\delta$ ):  $\delta$  8.8 (broad s, 1H, -OH), 5.215 (dd, <sup>2</sup>J(<sup>1</sup>H,<sup>1</sup>H) = 9.0 Hz, <sup>3</sup>J(<sup>1</sup>H,<sup>1</sup>H) = 5.9 Hz, 1H, H<sup>γ</sup>), 4.54 (m, 1H, H<sup>β</sup>), 4.183 (dd, <sup>2</sup>J(<sup>1</sup>H,<sup>1</sup>H) = 9.8 Hz, <sup>3</sup>J(<sup>1</sup>H,<sup>1</sup>H) = 9.8 Hz, 1H, H<sup>α</sup>), 3.896 (dd, <sup>2</sup>J(<sup>1</sup>H,<sup>1</sup>H) = 11.0 Hz, <sup>3</sup>J(<sup>1</sup>H,<sup>1</sup>H) = 7.0 Hz, 1H, H<sup>β</sup>), 3.302 (dd, <sup>2</sup>J(<sup>1</sup>H,<sup>1</sup>H) = 11.0 Hz, <sup>3</sup>J(<sup>1</sup>H,<sup>1</sup>H) = 11.0 Hz, 1H, H<sup>α</sup>). <sup>13</sup>C NMR (DMSO-*d*<sub>6</sub>, 25 °C;  $\delta$ ):  $\delta$  76.3 (-TeCH<sub>2</sub>-), 63.0 (-OCH<sub>2</sub>-), 56.1 (-CHCl-). <sup>125</sup>Te NMR (DMSO-*d*<sub>6</sub>, 70 °C;  $\delta$ ):  $\delta$  1416,  $\Delta\nu_{1/2}$  12400 Hz. IR (NaCl, Nujol; cm<sup>-1</sup>): 3433 vs  $\nu$ (O-H), 3012 m  $\nu_s$ (H<sub>2</sub>C<sub>Te</sub>), 2947 m  $\nu_s$ (H<sub>2</sub>C<sub>O</sub>), 2931 sh  $\nu$ (H<sub>2</sub>C<sub>Cl</sub>), 2895 w  $\nu_{as}$ (H<sub>2</sub>C<sub>Te</sub>), 2874 w  $\nu_{as}$ (H<sub>2</sub>C<sub>O</sub>), 2861 sh, 1457 m  $\delta$ (H<sub>2</sub>C<sub>O</sub>), 1400 s  $\delta$ (H<sub>2</sub>C<sub>Te</sub>), 1375 sh  $\delta$ (OH), 1343 m  $\delta$ (CH), 1316 m, 1253 m, 1220 w, 1100 sh, 1084 s, 995 vs  $\nu$ (C-O), 957 vs  $\nu$ (C-O), 894 ms  $\rho$ (H<sub>2</sub>C<sub>Te</sub>), 828 m  $\rho$ (H<sub>2</sub>C<sub>Te</sub>), 811 sh, 787 vs  $\nu$ (C-Cl), 668 w, 604 m, 551 s  $\nu$ (Te-O), 459 m. Crystals of **1** were grown by slow evaporation of the solvent from the CCl<sub>4</sub> solution, in which it was prepared. The identity of the crystals and the powdery solid was shown by comparison of their <sup>1</sup>H NMR spectra.

(27) Reed, A. E.; Weinstock, R. B.; Weinhold, F. *J. Chem. Phys.* **1985**, *83*, 735-746.

(28) Reed, A. E.; Curtiss, L. A.; Weinhold, F. *Chem. Rev.* **1988**, *88*, 899-926.

(26) MP2/LANL2DZP geometry optimizations and thermochemical calculations for **1** were beyond our computational limits.



Table 5. Crystal Data for Compounds **1** and **2**<sup>a</sup>

	<b>1</b>	<b>2</b>
empirical formula	C <sub>6</sub> H <sub>11</sub> O <sub>2</sub> Cl <sub>7</sub> Te <sub>2</sub>	C <sub>5</sub> H <sub>8</sub> O <sub>2</sub> TeCl <sub>4</sub>
fw	618.5	369.52
cryst syst	triclinic	monoclinic
space group	P1	P2 <sub>1</sub> /c
Z	2	4
temp/K	193	182
ρ <sub>calcd</sub> /g cm <sup>-3</sup>	2.484	2.141
cryst size/mm	0.20 × 0.05 × 0.05	0.2 × 0.14 × 0.09
a/Å	8.3139(8)	9.7632(6)
b/Å	8.8317(8)	8.1175(5)
c/Å	11.4338(10)	15.2195(9)
α/deg	88.059(2)	90.00
β/deg	82.235(2)	108.09(1)
γ/deg	83.783(2)	90.00
V/Å <sup>3</sup>	826.8(2)	1146.54(2)
no. of rflns measd	7249	10 256
no. of unique rflns	3853	2824
no. of params/restraints	172/0	109/0
range of transmissn	0.762–0.928	0.438–0.539
μ/cm <sup>-1</sup>	46.5	34.9
abs cor	MULABS <sup>32</sup>	MULABS <sup>32</sup>
R (I > 2σ(I)) <sup>b</sup>	0.0361	0.0306
GOF on F <sup>2</sup>	0.891	1.001
largest diff peak and hole/e Å <sup>-3</sup> c	1.115 and -1.213	0.819 and -0.711

<sup>a</sup> For both experiments, Mo Kα radiation with λ = 0.710 73 Å was used. <sup>b</sup> R = Σ||F<sub>o</sub> - |F<sub>c</sub>||/Σ|F<sub>o</sub>|. <sup>c</sup> The largest difference peak is about 1 Å from the Te atoms in both cases. The largest difference hole is about 1 Å from Te in **1** and about 1.2 Å from H6 in **2**.

Cl<sub>3</sub>Te[CH<sub>2</sub>CH(CH<sub>2</sub>Cl)OC(CH<sub>3</sub>)=O···] (**2**). **2** was prepared according to the literature procedure,<sup>6</sup> using CCl<sub>4</sub> instead of CHCl<sub>3</sub> as a solvent.

Yield: 88%. <sup>13</sup>C NMR (CDCl<sub>3</sub>; δ): 180.6 [-C(O)O-], 74.2 [-OCH(CH<sub>2</sub>Cl)-], 64.2 (-CH<sub>2</sub>Cl), 45.1(-TeCH<sub>2</sub>-), 21.7 (-CH<sub>3</sub>). <sup>125</sup>Te NMR (CDCl<sub>3</sub>; δ): 1400.1. IR (CsI, Nujol; cm<sup>-1</sup>): 3028 s ν(CH<sub>3</sub>), 3014 and 2998 s ν(H<sub>2</sub>C<sub>Te</sub>) and ν(H<sub>2</sub>C<sub>Cl</sub>), 2983 s ν(CH<sub>3</sub>), 2966 s ν(CH), 2940.0 s ν(H<sub>2</sub>C<sub>Cl</sub>), 2926.5 s ν(H<sub>2</sub>C<sub>Te</sub>), 1625.7 vs ν(C=O),<sup>29</sup> 1425.2 sh δ(H<sub>2</sub>C<sub>Cl</sub>), 1416.5 s δ(H<sub>2</sub>C<sub>Te</sub>) + δ(CH), 1046.2 s ν(C-O), 766 s ν(C-Cl), 340 s ν(Te-Cl), 262 s ν(Te-Cl).

From a saturated solution of **2** in CCl<sub>4</sub> kept at 5 °C, crystals suitable for single-crystal XRD were obtained within 3 days.

**Formation of 2 by Acetylation of 1.** In analogy to the procedure reported by Engman, acetyl chloride (220 mg, 2.77 mmol) was added to a stirred suspension of **1** (830 mg, 1.34 mmol) in 20 mL of CHCl<sub>3</sub>. The solid immediately dissolved on addition of acetyl chloride, and the solution was refluxed for 3 h. Then, all volatile compounds were removed in vacuo and a <sup>1</sup>H NMR spectrum was recorded from a sample of the brown, viscous residue, dissolved in CDCl<sub>3</sub>. Among other compounds, formation of **2** could be inferred. Subsequently, 20 mL of CHCl<sub>3</sub> was added to the residue and the solution refluxed for another 6 h. Again, the solvent was removed in vacuo and a <sup>1</sup>H NMR spectrum was recorded from a sample of the residue. The spectrum showed that the amount of **2** had significantly increased at the cost of the other, nonidentified intermediates.

(29) Engman<sup>6</sup> reported ν(C=O) 1610 cm<sup>-1</sup>.

**Crystal Structure Determination.** The crystal structure data were collected on a Siemens P4 diffractometer, and the structures were solved by direct methods and difference Fourier techniques (SIR);<sup>30</sup> structural refinement was against F<sup>2</sup> (SHELXL-97).<sup>31</sup> Details of the crystal structure determination of and the crystal data for **1** and **2** are given in Table 5.

**Theoretical Methods.** The ab initio calculations were performed on various servers of the Zentrum für Datenverarbeitung, Universität Mainz, using the GAUSSIAN94 software package.<sup>33</sup> The structures of all molecules investigated were fully optimized, followed by a numerical calculation of the vibrational frequencies from analytic first derivatives of the potential energy. Second-order perturbation calculations according to the theory of Møller and Plesset (MP2) followed the HF studies to account for effects of dynamic electron correlation.<sup>34</sup> With both levels an effective core double-ζ valence basis set according to Hay and Wadt<sup>35</sup> augmented by appropriate polarization functions for Te, Cl, O, and C (MP2/LANL2DZP) was used.<sup>36</sup> If not stated elsewhere, geometrical parameters and energies from MP2/LANL2DZP calculations are given. Geometry optimizations for **1**, **1A**, **1B**, and **2** started from XRD structures; for the 1,2-adduct of TeCl<sub>4</sub> with allyl acetate, reasonable bond lengths, bond angles, and torsion angles were such as to allow for an intermolecular Te···O interaction.

**Acknowledgment.** We thank Dr. Andreas Höfer, Institut für Anorganische Chemie und Analytische Chemie, Universität Mainz, for recording the low-temperature IR spectra and the Fonds der Chemischen Industrie for financial support (H.F.).

**Supporting Information Available:** Tables giving atomic coordinates, anisotropic thermal parameters, bond lengths, and bond angles, packing diagrams, and the crystallographic data, in CIF format, for the two structures presented in this paper. This material is available free of charge via the Internet at <http://pubs.acs.org>.

OM0104159

(30) Altomare, A.; Cascarano, G.; Giacovazzo, C.; Guagliardi, A.; Burla, M. C.; Polidori, G.; Camalli, M. SIR-A Program for the Automatic Solution of Crystal Structures by Direct Methods. *J. Appl. Crystallogr.* **1994**, *27*, 435–436.

(31) Sheldrick, G. M. SHELXL-97: Program for Crystal Structure Refinement; Universität Göttingen, Göttingen, Germany, 1997.

(32) Blessing, R. *Acta Crystallogr.* **1995**, *A51*, 33–38.

(33) Frisch, M. J.; Trucks, G. W.; Schlegel, H. B.; Gill, P. M. W.; Johnson, B. G.; Robb, M. A.; Cheeseman, J. R.; Keith, T.; Petersson, G. A.; Montgomery, J. A.; Raghavachari, K.; Al-Laham, M. A.; Zakrzewski, V. G.; Ortiz, J. V.; Foresman, J. B.; Cioslowski, J.; Stefanov, B. B.; Nanayakkara, A.; Challacombe, M.; Peng, C. Y.; Ayala, P. Y.; Chen, W.; Wong, M. W.; Andres, J. L.; Replogle, E. S.; Gomperts, R.; Martin, R. L.; Fox, D. J.; Binkley, J. S.; Defrees, D. J.; Baker, J.; Stewart, J. P.; Head-Gordon, M.; Gonzalez, C.; Pople, J. A. *Gaussian 94*, revision E.2; Gaussian, Inc.: Pittsburgh, PA, 1995.

(34) For the terminology of computational chemistry, see e.g.: Hehre, W. J.; Radom, L.; Schleyer, P. v. R.; Pople, J. A. *Ab Initio Molecular Orbital Theory*; Wiley: New York, 1986.

(35) Wadt, W. R.; Hay, P. J. *J. Chem. Phys.* **1985**, *82*, 284–298.

(36) Höllwarth, A.; Böhme, M.; Dapprich, S.; Ehlers, A. W.; Gobbi, A.; Jonas, V.; Köhler, K. F.; Stegmann, R.; Veldkamp, A.; Frenking, G. *Chem. Phys. Lett.* **1993**, *208*, 237–240.